

## Reduction of the Mesoscopic Conductance-Fluctuation Amplitude in GaAs/AlGaAs Heterojunctions Due to Spin-Orbit Scattering

O. Millo, S. J. Klepper, M. W. Keller, D. E. Prober, S. Xiong, and A. D. Stone

*Departments of Applied Physics and Physics, Yale University, New Haven, Connecticut 06520*

R. N. Sacks

*United Technologies Research Center, East Hartford, Connecticut 06108*

(Received 11 July 1990)

We have studied weak localization and conductance fluctuations in 2D mesoscopic GaAs/AlGaAs heterojunctions for  $T=60$  mK to 7 K. The weak-localization data show that the spin-orbit scattering rate exceeds the phase-breaking rate below  $\sim 2$  K. At the same time, the conductance-fluctuation amplitude is reduced significantly below  $\sim 2$  K, as compared to that extrapolated from the high-temperature region. Our data agree well with calculations for the effect of spin-orbit scattering on the conductance-fluctuation amplitude. A related effect on the magnetic correlation field is also discussed.

PACS numbers: 72.20.My, 73.20.Fz, 73.40.Kp

Universal conductance fluctuations<sup>1</sup> (UCF) are a novel quantum interference effect in small weakly random systems. These are manifest as reproducible, but sample-specific, conductance fluctuations as a function of magnetic field<sup>2</sup> or chemical potential.<sup>3</sup> At zero temperature, the rms UCF amplitude  $\delta G$  is of order  $e^2/h$ , independent of sample size and degree of disorder. UCF clearly demonstrate the importance of electron phase coherence at low temperatures. Much recent attention has been focused on the effects of spin-orbit (SO) scattering and magnetic field on  $\delta G$ , due to the connection of these effects to random-matrix theories (RMT).<sup>4,5</sup> These theories treat quantum transport on the basis of "universality classes" of random Hamiltonians. The ratios of  $\delta G$  for Hamiltonians in different universality classes follow from very general symmetry principles and are independent of microscopic details of the system. Both random-matrix<sup>4,5</sup> and diagrammatic<sup>1,6,7</sup> theories predict that as long as the magnetic field does not cause significant Zeeman splitting,  $H < H_Z = k_B T / g\mu_B$  is reduced by a factor of 2 in the presence of strong SO scattering, as compared to the amplitude for an identical system, at the same field, having negligible SO scattering. The diagrammatic theory attributes this factor-of-2 reduction to the suppression of the contribution of the triplet terms to the conductance fluctuations in both the Cooper and the diffusion channels. Within the RMT approach, at zero magnetic field the factor-of-2 reduction is due to a transition from the orthogonal to the symplectic ensemble. At "moderate" magnetic fields,  $H < H_Z$  but sufficiently large to suppress the Cooper channel, this reduction is due to breaking of spin degeneracy, which increases level repulsion. These reductions are summarized in Table I. The theories also predict reduction factors in  $\delta G$  due to magnetic fields. These are also shown in Table I, and have been observed in experiment.<sup>3,8,9</sup> The direct effect of SO scattering on UCF has not yet been established experimentally.

In this Letter we report the observation of a reduction in the UCF amplitude due to SO scattering. In our GaAs/AlGaAs heterojunctions the SO scattering length  $L_{SO}$  is shorter than the phase-breaking length  $L_\phi$ , below  $\sim 2$  K and is shorter than the thermal diffusion length  $L_T$  below  $\sim 0.3$  K. Thus, by changing the temperature we cross from a weak SO regime (high  $T$ ) to a strong SO regime (low  $T$ ). At the same time, the UCF amplitude at lower temperatures is reduced with respect to that extrapolated from the high-temperature regime. The main advantage of our experimental system is that the transition from the weak to the strong SO regime is done within a *single* sample; i.e., we do not need to dope with impurities having large SO scattering potentials. A critical feature of the GaAs/AlGaAs heterojunctions for this work is that the impurities are *not* mobile<sup>3</sup> at the temperatures employed, in contrast to the situation in metal films.<sup>8</sup>

We fabricated two-dimensional mesoscopic<sup>1</sup> devices from modulation-doped, molecular-beam epitaxy grown  $\text{Al}_{0.3}\text{Ga}_{0.7}\text{As}/\text{GaAs}$  heterojunctions. We omitted the usual undoped spacer layer. The mobility is thus fairly low, and electron transport is diffusive.<sup>1</sup> The results presented here were obtained from two different samples. The first, sample *A*, is a  $L \times W \sim 10 \times 7 \mu\text{m}^2$  sample, having sheet resistance  $R_\square \approx 220 \Omega$ , electron density  $n \approx 9 \times 10^{11} \text{cm}^{-2}$  (we tested that only the first subband was populated), mobility  $\mu \approx 30000 \text{cm}^2/\text{Vs}$ , diffusion

TABLE I. Conductance-fluctuation amplitude  $\delta G$  normalized to the weak SO and  $H=0$  case (see text). In our system  $H_1 = \Phi_0/L_T^2$ ;  $\Phi_0$  is the flux quantum  $h/e$  and  $L_1 = \sqrt{\hbar D/k_B T}$ .

	$H=0$	$H$ moderate $H_1 < H < H_Z$	$H$ strong $H > H_Z$
Weak SO	1	$1/\sqrt{2}$	$1/2$
Strong SO	$1/2$	$1/2\sqrt{2}$	$1/2\sqrt{2}$

constant  $D \approx 1000 \text{ cm}^2/\text{s}$ ,  $L_T = \sqrt{\hbar D/k_B T} \approx 0.9 \text{ } \mu\text{m}$  at 1 K, and elastic mean free path  $l \approx 0.4 \text{ } \mu\text{m}$ . This sample was measured at  $T \geq 0.4 \text{ K}$  in pumped  $^3\text{He}$  and  $^4\text{He}$  systems. Sample *B* was measured also in a dilution refrigerator down to 60 mK. It is a  $\sim 15 \times 15\text{-}\mu\text{m}^2$  device having  $R_{\square} \approx 300 \text{ } \Omega$  and  $n \approx 9.5 \times 10^{11} \text{ cm}^{-2}$ . The conductance-fluctuation measurements were made by a standard four-terminal ac measurement, while the low-field weak-localization data were obtained using a four-terminal ac bridge. The ac drive currents were 40 nA for sample *A* and 5 nA for sample *B* at the lowest temperature, small enough to avoid self-heating.

In the inset of Fig. 1 we plot two low-field magnetoresistance traces,  $\Delta R = R(H) - R(0)$ , taken for sample *A* at two different temperatures. These are normalized by the zero-field resistance. The  $T=6 \text{ K}$  trace shows negative magnetoresistance only, which indicates that SO scattering is relatively weak.<sup>10</sup> The  $T=1.5 \text{ K}$  trace, on the other hand, shows positive magnetoresistance below 2 G, indicating that the SO scattering rate  $\tau_{\text{SO}}^{-1}$  exceeds the phase-breaking rate  $\tau_{\phi}^{-1}$ . By fitting the 2D weak-localization theory<sup>10</sup> to the symmetric part (with respect to the magnetic field) of such traces, we obtain  $L_{\phi} = \sqrt{D\tau_{\phi}}$ , and  $L_{\text{SO}} = \sqrt{D\tau_{\text{SO}}}$ . The fittings are done over a very narrow field range, 0–8 G, since the theory applies only up to the “elastic field,”  $\hbar/8\pi el^2$ , which is  $\sim 10 \text{ G}$  in our devices.  $L_{\phi}$  and  $L_{\text{SO}}$  are plotted in Fig. 1, together with  $L_T$ , as functions of  $T^{-1/2}$ . Figure 1 shows that  $\tau_{\phi}^{-1}$

is proportional to  $T$ , indicating that the dominant phase-breaking mechanism is electron-electron scattering in a dirty 2D system.<sup>11</sup> Indeed,  $L_{\phi}(1 \text{ K}) \approx 2.4 \text{ } \mu\text{m}$  yields  $\tau_{\phi}^{-1} \approx 1.6 \times 10^{10} \text{ s}^{-1}$  at 1 K, in fair agreement with the calculation of Altshuler and co-workers,<sup>11</sup> which gives  $\tau_{\phi}^{-1} \sim 0.7 \times 10^{10} \text{ s}^{-1}$ . The fact that  $L_{\phi}$  does not deviate from the  $T^{-1/2}$  behavior indicates that self-heating is negligible. Figure 1 shows also that  $L_{\text{SO}} \approx 1.7 \text{ } \mu\text{m}$  is nearly independent of  $T$ , as expected.<sup>12</sup>  $L_{\text{SO}}$  is shorter than  $L_{\phi}$  below 2 K, and shorter than  $L_T$  below 0.3 K. Sample *B* showed similar behavior. There,  $L_{\text{SO}} \approx 1.5 \text{ } \mu\text{m}$ ,  $L_{\phi}(1 \text{ K}) \approx 1.7 \text{ } \mu\text{m}$ ,  $L_{\phi} > L_{\text{SO}}$  below 1.2 K, and  $L_T > L_{\text{SO}}$  below 0.3 K.

The reason for the relatively strong SO scattering in our devices, as compared to that typically reported for AlGaAs/GaAs heterojunctions,<sup>3,9</sup> is our high electron density. In recent experiments<sup>12</sup> it was found that  $\tau_{\text{SO}}^{-1} \propto n^3$ , a fact which is attributed<sup>12</sup> to a band-structure mechanism for the SO scattering, due to the strong crystal fields in the polar GaAs crystal. A consequence of the strong SO scattering is that in our system Zeeman splitting exceeds the SO energy only at magnetic fields larger than  $\hbar \tau_{\text{SO}}^{-1} |g| \mu_B \approx 9 \text{ kG}$ , taking<sup>13</sup>  $g = -0.44$ . We do not exceed 3 kG in our experiment.

In Fig. 2 we plot the rms conductance-fluctuation amplitude normalized to the average conductance  $\delta G / \langle G \rangle$

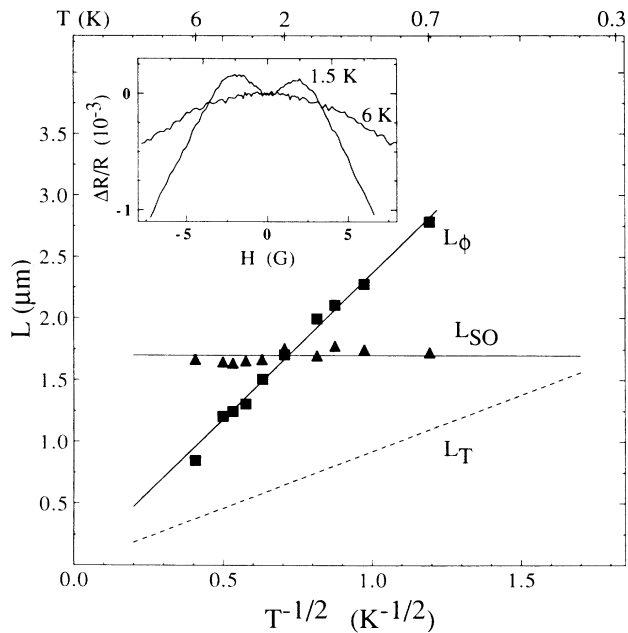


FIG. 1. Phase-breaking (squares), spin-orbit scattering (triangles), and thermal (dashed line) lengths as functions of  $T^{-1/2}$ ; sample *A*. These were calculated from traces such as those shown in the inset for 1.5 and 6 K. Solid lines represent least-squares fits to the data.

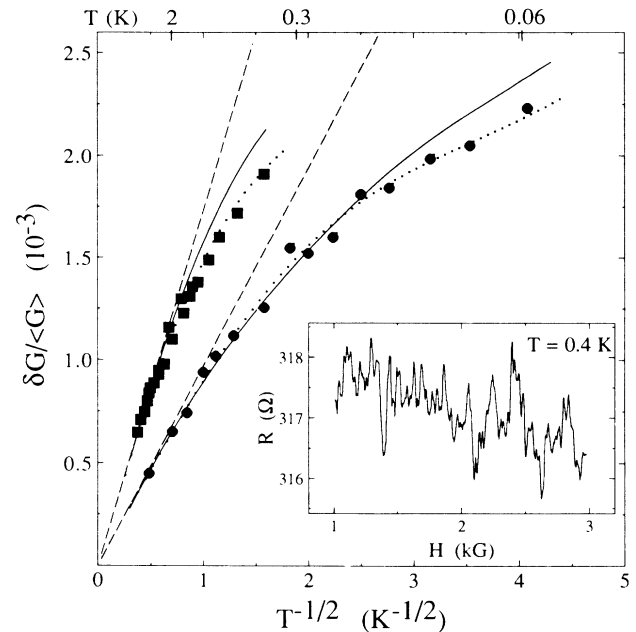


FIG. 2. The rms amplitude of the conductance fluctuations  $\delta G$  normalized to the average conductance for sample *A* (squares) and sample *B* (circles) vs  $T^{-1/2}$ .  $\delta G$  was calculated from traces such as the one shown in the inset for sample *A* at 0.4 K. Dashed lines extrapolate the high-temperature data, Eq. (1). Solid curves represent diagrammatic calculations multiplied by  $\sim 0.8$  to fit the high- $T$  data. Dotted curves were calculated from Eq. (3), as explained in the text.

as a function of  $T^{-1/2}$ .  $\delta G$  was calculated from magnetoresistance traces taken between 1 and 3 kG, such as the one shown in the inset for sample *A* at 0.4 K. The squares and circles represent data obtained from samples *A* and *B*, respectively. At high temperatures  $\delta G$  is characterized by a  $T^{-1/2}$  dependence. This is a consequence of thermal and spatial averaging in the regime of weak SO scattering.<sup>1</sup> In our case, where  $L_T$  and  $L_\phi$  are both proportional to  $T^{-1/2}$ , theory estimates for this high-temperature regime<sup>1</sup>

$$\delta G/\langle G \rangle = C(e^2/h)R_\square(2\pi\hbar D/k_B L W)^{1/2} T^{-1/2}, \quad (1)$$

where  $C$  is a constant of order unity which depends on magnetic field and on the ratio  $L_\phi/L_T$ . Experimentally we find  $C=0.73$  and  $0.63$  for samples *A* and *B*, respectively.  $R_\square$  is nearly independent of temperature in the range of magnetic field used. At lower temperatures, there is a significant reduction of the amplitude as compared to that extrapolated (dashed lines) from the high-temperature region. In sample *A* the reduction starts at  $\sim 2$  K, while in sample *B* it starts at  $\sim 1$  K. This is consistent with the crossover temperatures observed in our weak-localization experiments, and is further discussed below.

The solid curves in Fig. 2 represent results of a diagrammatic calculation. First, we calculate the diffusion pole, in a fashion similar to that in Ref. 1, and obtain

$$D_{J,M}(n,m,\Delta E,H) = \{n^2 + S^2 m^2 + (L/\pi L_\phi)^2 + (4J/3)(L/\pi L_{SO})^2 + i[\Delta E + Mg\mu_B H]/\pi^2 E_c\}^{-1}, \quad (2)$$

where  $J$  and  $M$  are the total spin of the diffusion and its  $z$  component, respectively,  $n$  and  $m$  are integers,  $S=L/W$ ,  $\Delta E$  is the energy difference between the two Green's functions in the diffusion propagator, and  $E_c = \hbar D/L^2$  is the energy correlation range.<sup>1</sup> (Note that the Zeeman term, though small, is included.) It can be seen from Eq. (2) that only the triplet ( $J=1$ ) terms are suppressed by the SO interaction. Next, we calculate  $\delta G$  using Eq. (4) of Ref. 6 with the diffusion pole given above. In the computation, we take our experimental values for  $L_\phi$ ,  $L_{SO}$ , and  $D$ . For the Zeeman term we use<sup>13</sup>  $g = -0.44$  and a magnetic field  $H=2$  kG, being the average value used. The Cooper pole is not calculated, since it is suppressed at the magnetic fields employed.<sup>1,4,6</sup> We multiply our theoretical result for  $\delta G$  by a numerical factor to fit the high-temperature experimental data. Note that this is the *only* adjustable parameter in this calculation, which, for *both* samples, is  $\sim 0.8$ . This agreement in the high-temperature regime is significant in itself; this is the first time that a complete diagrammatic calculation which includes thermal averaging has been compared with experiment. The calculation also fits the reduction effect rather well, as shown in Fig. 2.

A theoretical study of the effect of SO scattering on the conductance of one-dimensional rings was presented

by Meir, Gefen, and Entin-Wohlman.<sup>14</sup> In their picture, the SO interaction affects the magnetoconductance by inducing an effective flux, having opposite signs for the two different spin directions. Extending their discussion to bulk systems, they derived a general relation between the SO-induced reductions of  $\delta G$  and  $\langle G \rangle$ . Using a semiclassical result for the latter,<sup>15</sup> they obtain

$$\delta G/\delta G_0 = 0.5\{3\exp(-4L_c^2/3L_{SO}^2) + 1\}^{1/2}, \quad (3)$$

where  $\delta G_0$  is the magnitude of  $\delta G$  with no SO scattering (i.e., the dashed lines in Fig. 2) and  $L_c$  is a characteristic length. We assume that  $L_c \approx L_T$ , the shorter of the two cutoff lengths in the UCF theory,  $L_\phi$  and  $L_T$ . Taking  $L_c = 1.12L_T$  and  $L_c = 0.65L_T$  for samples *A* and *B*, respectively, we obtain best fits of Eq. (3) to our experimental data. These are represented by the dotted curves in Fig. 2. Note that because of the semiclassical approximation<sup>15</sup> taken, Eq. (3) is not exact. The fact that the dotted curves fit the data so well is due to Eq. (3) having essentially two adjustable parameters,  $\delta G_0$  and  $L_c$ . We therefore do not claim that the agreement with the data is definitive. Nevertheless, Eq. (3) and its fits to the data, with reasonable values for  $L_c$ , do serve as a useful way to visualize the SO-induced reduction in  $\delta G$ .

At the lowest temperature for sample *A*, 0.4 K, the reduction factor in the UCF amplitude is  $\sim 0.7$ , which is still not the full effect (0.5 reduction). Because of thermal averaging,<sup>1</sup> the full reduction is expected to be observed in both samples only for  $T \ll 0.3$  K, where  $L_T \gg L_{SO}$  (see Fig. 1). Indeed, the data obtained from sample *B* reach a reduction of  $\sim 0.6$  at a temperature where  $L_T \approx 2L_{SO}$ . We note that the observed reduction cannot be attributed to a dimensional crossover, since both samples have width  $\approx 2L_\phi$  at the lowest temperature. We also note that the magnetic fields used were clearly in the moderate regime (see Table I) for  $T > 0.1$  K. The possible crossover to the  $H > H_Z$  regime for sample *B* below 0.1 K should not by itself reduce  $\delta G$  any further, since we are in the regime of strong SO scattering.

Finally, we discuss the temperature dependence of the magnetic correlation field  $H_c$ , which is the typical spacing of the fluctuations versus magnetic field.<sup>1</sup>  $H_c$  is shown for sample *A* in Fig. 3. The data for  $T > 2.5$  K show a clear linear dependence of  $H_c$  on temperature, which extrapolates (solid line) to  $H_c = 0$  at zero temperature. Below 2 K,  $H_c$  is larger than this extrapolation. In order to understand the data, we recall that the cutoff length of the triplet terms,  $L_2$ , is given<sup>7,10,16</sup> by  $L_2^{-2} = L_T^{-2} + \frac{4}{3}L_{SO}^{-2}$  in systems where  $L_T < L_\phi$ . The singlet term has a cutoff length  $L_T$ . The correlation fields for the triplet and singlet terms are, respectively,  $H_c^t \propto \Phi_0 L_2^{-2}$  and  $H_c^s = H_{c0} \propto \Phi_0 L_T^{-2} \propto T$ , where  $H_{c0}$  is the correlation field in the absence of SO scattering and  $\Phi_0$  is the flux quantum  $h/e$ . At high temperatures,  $L_2 \approx L_T$ ;  $H_c^t$  approaches  $H_{c0}$ , so that the net  $H_c$ , for the singlet and triplet terms together, is just  $H_{c0}$ . At 0.4 K,

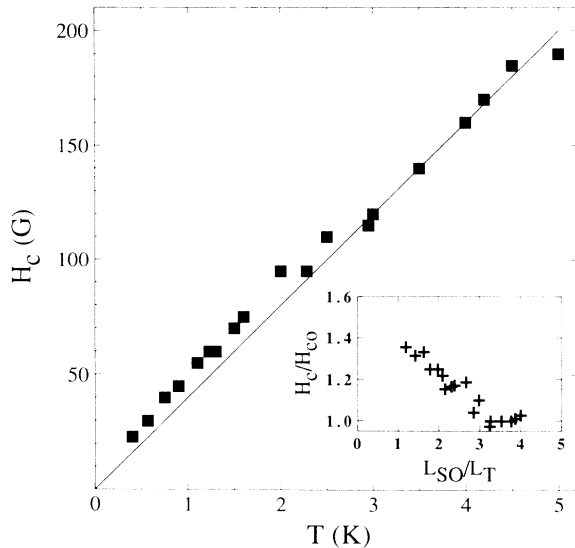


FIG. 3. Magnetic-field correlation range  $H_c$  as a function of  $T$  for sample  $A$ . The line extrapolates from the high-temperature region. Inset: Enhancement of  $H_c$  over the value  $H_{c0}$  expected from the high-temperature extrapolation vs the ratio of the SO length to the thermal length.

$L_{SO} \approx L_T$ ; thus  $H_c^i > H_{c0}$ , and so  $H_c$  is enhanced over  $H_{c0}$ .<sup>16</sup> (At yet lower temperatures, the contribution of the triplet terms to the conductance will be negligible;  $H_c$  is then expected again to approach  $H_{c0}$ .) In the inset of Fig. 3 we plot the enhancement  $H_c/H_{c0}$  as a function of  $L_{SO}/L_T$ . For  $H_{c0}$ , we take the high-temperature extrapolation. Recently, Chandrasekhar, Santhanam, and Prober<sup>16</sup> calculated the enhancement  $H_c/H_{c0}$  for a 1D sample. They found it to peak at a value of  $\sim 1.2$ . Our data agree qualitatively with their results.

In conclusion, we have observed a SO-induced reduction of the rms UCF amplitude  $\delta G$ . Our data agree well with theoretical calculations for this effect. The temperature dependence of  $H_c$  can also be understood as due to the effect of SO scattering.

We are grateful to P. D. Dresselhaus, C. A. Richter, and R. G. Wheeler for useful discussions, and for assistance with their  $^3\text{He}$  system, and to M. A. Kastner, U. Meirav, and J. Scott-Thomas for their help and hospitality when using their dilution refrigerator. Discussions with Y. Meir and V. Chandrasekhar are also acknowledged. This work was supported by NSF Grants No. DMR-8505539 and No. DMR-8658135 and by a Weizmann Fellowship to one of us (O.M.)

<sup>1</sup>P. A. Lee, A. D. Stone, and H. Fukuyama, Phys. Rev. B **35**, 1039 (1987), and references therein.

<sup>2</sup>C. P. Umbach *et al.*, Phys. Rev. B **30**, 4048 (1984).

<sup>3</sup>P. Debray *et al.*, Phys. Rev. Lett. **63**, 2264 (1989).

<sup>4</sup>B. L. Altshuler and B. I. Shklovskii, Zh. Eksp. Teor. Fiz. **91**, 220 (1986) [Sov. Phys. JETP **64**, 127 (1986)].

<sup>5</sup>Y. Imry, Europhys. Lett. **1**, 249 (1986); K. A. Muttalib, J.-L. Pichard, and A. D. Stone, Phys. Rev. Lett. **59**, 2475 (1987); P. A. Mello, Phys. Rev. Lett. **60**, 1089 (1988).

<sup>6</sup>A. D. Stone, Phys. Rev. B **39**, 10736 (1989).

<sup>7</sup>S. Feng, Phys. Rev. B **39**, 8722 (1989).

<sup>8</sup>N. O. Birge, B. Golding, and W. H. Haemmerle, Phys. Rev. Lett. **62**, 195 (1989).

<sup>9</sup>D. Mailly *et al.*, Europhys. Lett. **8**, 471 (1989).

<sup>10</sup>S. Hikami, A. I. Larkin, and Y. Nagaoka, Prog. Theor. Phys. **63**, 707 (1980); G. Bergmann, Phys. Rep. **107**, 1 (1984).

<sup>11</sup>B. L. Altshuler, A. G. Aronov, and D. E. Khmel'nitskii, J. Phys. C **15**, 7367 (1982); B. L. Altshuler and A. G. Aronov, Solid State Commun. **46**, 429 (1983).

<sup>12</sup>C. A. Papavassiliou, P. D. Dresselhaus, and R. G. Wheeler, Bull. Am. Phys. Soc. **33**, 806 (1988); (private communication).

<sup>13</sup>D. Stein, K. von Klitzing, and G. Weimann, Phys. Rev. Lett. **51**, 130 (1983).

<sup>14</sup>Y. Meir, Y. Gefen, and O. Entin-Wohlman, Phys. Rev. Lett. **63**, 798 (1989).

<sup>15</sup>S. Chakravarty and A. Schmid, Phys. Rep. **140**, 193 (1986).

<sup>16</sup>V. Chandrasekhar, P. Santhanam, and D. E. Prober (to be published).